Radioactivation Analysis of Concrete Wall in OKTAVIAN Facility

Shingo TAMAKI, Fajar PANUNTUN[1)], Kazumichi UEDOI, Wang HAIDONG, Sachie KUSAKA, Yuichiro MANABE, Yoko AKIYAMA, Teruya TANAKA[2)], Fuminobu SATO and Isao MURATA

Graduate School of Engineering, Osaka University, 2-1 Yamadaoka, Suita, Osaka 565-0871, Japan
[1)]*National Nuclear Energy Agency of Indonesia, Jl. Kuningan Barat, Mampang Prapatan Jakarta, 12710, Indonesia*
[2)]*National Institute for Fusion Science, Toki 509-5292, Japan*

(Received 15 August 2021 / Accepted 18 November 2021)

A deuterium-tritium (DT) neutron generator in Osaka University with a continuous intense neutron source emitting 3×10^{12} fusion neutrons per second has been in operation since 1981. However, radioactivation for the parts of the accelerator body is a serious issue. Hence, in this study, we investigated the radioactivation of the intense irradiation room containing the continuous intense neutron source. Core samples of the concrete wall were collected at various positions in the irradiation room and the radionuclides in them were determined by performing gamma-ray spectrometry. Major long-lived radionuclides found were ^{54}Mn, ^{60}Co, and ^{152}Eu. The radioactivity of ^{152}Eu may possibly be consistent with the result obtained using the simulation code. The radioactivities of ^{54}Mn and ^{60}Co were minimal compared with that of ^{152}Eu. The tritium amount in the core sample was measured employing a tritium sampling system and a liquid scintillation detector and was found to be considerably larger than the amount estimated using the simulation code. Tritium diffused from the titanium-tritium target was attached to the wall surface. However, most of it did not penetrate the concrete wall. These results reveal the radioactivity issue of fusion neutron generator facilities and are expected to aid in the maintenance of their operation.

Keywords: OKTAVIAN, fusion neutron, radioactivation, radioactive waste, tritium, ^{60}Co, ^{152}Eu

DOI: 10.1585/pfr.17.1405001

1. Introduction

Fusion reactors do not produce transuranium elements in contrast to fission reactors. However, fast neutrons produced in deuterium-tritium (DT) and deuterium-deuterium (DD) reactions induce radioactivity in a fusion reactor facility and the radioactivity depends on the composition of materials, neutron flux, and periods of exposure [1–5]. Studies on fusion reactor engineering have been conducted for decades. Consequently, many of the facilities where they have been conducted are very old with a few being shut down, and the problem of radioactivity in neutron generation facilities has become a critical issue. For example, Fusion Neutron Source (FNS) in Japan atomic energy agency (Japan), which had been in operation since 1981 was shut down in February 2016 [6]. Unfortunately, decommission process in FNS has been encountering problems because of the radioactivation of the facility components. Further, SNEG-13 in D. V. Efremov Institute of Electrophysical Apparatus (Russia), in operation since 1986 [7], and Frascati Neutron Generator in ENEA Frascati Research Center (Italy), since 1992 [8], are a few other important sites with still available fusion neutron sources. However, activated materials produced at old neutronics facilities approximately or greater than 30 years in operation, are expected to encounter problems similar that that in FNS. Moreover, radioactivation data in such facilities may aid in predicting the radioactivity in upcoming fusion reactors. Therefore, the estimation of radioactivity is significant to the reduction of radiological hazards for the decommission of such facilities and future fusion reactors.

An accelerator-based neutron generator, OKTAVIAN, was built at Osaka University in 1978 and has been in operation for approximately 40 years [9]. The continuous neutron source with 3×10^{12} DT neutrons per second was set in the intense irradiation room. The OKTAVIAN has been primarily devoted to engineering related to fusion neutrons. The maximum annual operating time was more than 1000 hours with no special maintenance difficulty. This facility comprises two irradiation rooms: a large irradiation room for DT pulsed neutron experiment and an intense irradiation room for strong continuous neutron field generation. The test operation of the nanosecond DT pulsed neutron source was performed in 1981. The final test of continuous deuterium ion beam at 30 mA was completed in 1982. Since then, the OKTAVIAN has continued to operate up till 2021. Therefore, the radioactivation issues have been considered to maintain the facility through partial modification and parts replacement. The radioactivation of parts around the neutron source of the accelerator body is inevitable, owing to high neutron fluence over a long period. For example, the dose rate when

author's e-mail: tamaki@see.eng.osaka-u.ac.jp

not in operation, in the vicinity of the neutron source target, has been determined to be over 1 μSv/h, and the radioactivity of the OKTAVIAN beam line has been measured using a survey meter. Subsequently, the radioactivity of ^{60}Co was approximately estimated considering the conversion factors to be over 2 Bq/g [10]. Further, the accelerator body is strongly contaminated with tritium. Moreover, information regarding the radioactivation of concrete walls in terms of both cost and volume is required. This study describes the radioactivation analysis of a concrete wall for the intense irradiation room in the OKTAVIAN. Core samples of the concrete wall were collected at various positions in the intense irradiation room and primary residual radionuclides were analyzed via gamma-ray spectrometry employing a high-purity Ge detector. The amount of tritium in the core sample was measured with a tritium sampler system and a liquid scintillation detector and the results of the main radionuclides were compared to those calculated using a neutron transport simulation code.

Previous studies have reported major radionuclides in certain particle accelerator facilities [11–22]. Major long-lived radionuclides include ^{3}H (T), ^{22}Na, ^{41}Ca, ^{45}Ca, ^{54}Mn, ^{55}Fe, ^{60}Co, ^{152}Eu, and ^{154}Eu. The ones that are particularly important and present in the concrete are T, ^{60}Co, and ^{152}Eu. The radionuclides of ^{60}Co are generated by thermal neutron capture reactions, whereas those of ^{152}Eu in concrete are based on ^{151}Eu(n,γ)^{152}Eu for thermal neutrons and ^{153}Eu(n,2n)^{152}Eu for fast neutrons. Further, the tritium production is based on fast and thermal neutron reactions such as ^{7}Li(n,n'α)T and ^{6}Li(n,α)T. In the OKTAVIAN, the concrete wall had been contaminated with tritium from titanium-tritium (Ti-T) targets.

2. OKTAVIAN Facility

Figure 1 shows the layout of the OKTAVIAN facility [9]. All major parts of the OKTAVIAN are installed in an 18 m × 32 m room, surrounded by concrete shielding walls. A deuterium ion beam with the energy of 300 keV is obtained using a Cockcroft-Walton type accelerator with a duoplasmatron ion source. After acceleration, two beamlines are provided through the switching magnet: one at the 37.5° line for continuous neutron source in the intense irradiation room, another at the 30° line for a pulsed neutron source. The maximum intensity of the continuous neutron source was approximately 3×10^{12} DT neutrons per second, and that of the pulsed neutron source was 10^{3} DT neutrons per pulse, with a duration of 1.5 ns. Fourteen MeV neutrons were generated by DT reactions, for which the deuterium ion beam was incident on the Ti layer occluding a large amount of tritium on a copper-backed plate. A rotating Ti-T target was used for the continuous neutron source until 1990. At present, water-cooled, fixed targets for the continuous neutron are being used. The intense irradiation room is surrounded by concrete shielding walls. Steps to prevent the spread of tritium contamination in and outside

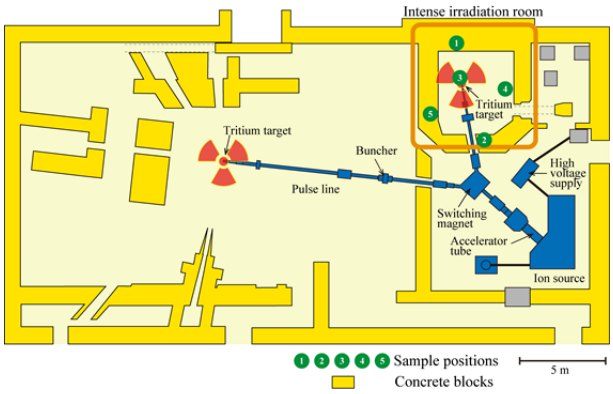

Fig. 1 Layout of the facility of the OKTAVIAN. The OKTAVIAN is an accelerator-based neutron generator. The deuterium ion beam is obtained using the Cockcroft-Walton type accelerator with a duoplasmatron ion source. Fourteen MeV neutrons are generated by a DT reaction, wherein the deuterium ion beam is incident on the Ti-T layer. The maximum intensity of the continuous neutron source in the intense irradiation room is 3×10^{12} neutrons per second.

of the facility have been taken. A two-stage tritium recovery system has been installed: the primary part is close to the rotating Ti-T target, where high tritium contamination is expected and a cause for concern. The recovery principle is based on hydrogen gas pumping by titanium getter pumps, while the secondary part is based on hydrogen gas oxidation by a palladium catalyzer doped with aluminum silicate and on the consequent water absorption by a molecular sieve.

Tables 1 and 2 show the maximum and daily operation parameters of OKTAVIAN [9]. For the continuous beamline, a 3×10^{13} Bq Ti-T target was used as a rotating target in the intense irradiation room. The research results have been provided to improve the evaluated nuclear data files and develop the calculation methods for the fusion reactor design. In addition, fast neutron irradiation experiments for fusion related material have also been used with the continuous DT neutrons. The damage caused by the DT neutrons to the optical and electronic instruments have been researched. The maximum annual operating time was 1000 hours. Furthermore, many fusion neutron experiments with the pulsed neutron source have been performed to study the fusion neutron transport characteristics, such as double-differential cross-section measurements and tritium breeding ratio measurements.

Figure 2 shows the amount of generated DT neutrons per year in the intense irradiation room estimated from the operation records of the continuous neutron source. The year of maximum neutron generation was 1989, following which the amount of time of the continuous neutron source has decreased significantly. From 1998 to 2015, the pulsed neutron source was mainly used to research double-differential cross-section measurements. Since

Table 1 Maximum and daily operation parameters of OKTAVIAN. For the continuous beam line, a 3×10^{13} Bq Ti-T target was used for a rotating target in the intense irradiation room. The maximum intensity of the continuous neutron source is 3×10^{12} neutrons per second.

	Maximum	Daily
Beam energy (keV)	300	250
D^+ beam current at rotating target (mA)	20	10
Minimum beam spot size at the target (mm)	15	~30
Rotating target diameter (cm)	20	~20
D-D neutron yield, continuous (n/s)	3×10^{10}	No use
D-T neutron yield, continuous (n/s)	3×10^{12}	10^{12}
Tritium amount for one rotating target (Bq/piece)	3×10^{13}	1×10^{13}
Target life (half value of neutron yield) (A h)	~1 A h for half-life	

Table 2 Maximum and daily operation parameters of OKTAVIAN for the pulse beam line.

	Maximum	Daily
Beam energy (keV)	300	245
Minimum beam spot size at the target (mm)	15	~30
Target life (half value of neutron yield) (A h)	~1 A h for half-life	
Pulse width (ns)	1.5	1.8
Ratio of neutron pulse/peak and background	10^4	5×10^3
D-T neutron yield of nanosecond pulsed mode (n/pulse)	$\sim10^4$	10^3

2016, water-cooled, fixed Ti targets with 3×10^{11} Bq tritium have been used in the continuous neutron source. The OKTAVIAN was not in operation from 2018 and 2020, owing to the malfunction caused by an earthquake of 6.1 Mj on June 18th, 2018. Following repairs in 2020, it has been in operation ever since.

3. Simulation for Radioactivity

A Monte Carlo particle transport simulation code, PHITS, was used to estimate the neutron transport and the radioactivity induced by DT neutrons [23]. PHITS simulates the production of the scattered neutrons and the nuclear interactions with nuclei of the material. In this study, default nuclear data library installed in PHITS, JENDL-4.0, and other data libraries were used to perform the simulation. Residual radionuclides were estimated using a DCHAIN-SP code and the tally of t-product in the PHITS. The DT neutron source was assumed to be emitted in a uniform direction, although DT neutron generation exhibits a slight angular dependence on the axis of the deuterium ion beamline. In addition, neutrons generated by the DD fusion reactions at the beam slits and beam dampers in the accelerator were ignored, owing to the low cross-section of DD reactions. The total generated DT neutrons with 14 MeV were used from the data in Fig. 2.

The elements in the concrete and accelerator components for the PHITS simulation are shown in Tables 3 and 4. The concentrations of certain major concrete elements were cited from that of standard concrete elements [24]. In particular, the concentrations of the minor elements Li, B, Mn, Co, Ni, Cs, Eu, and Gd were determined via induc-

Table 3 Elements in the concrete for the PHITS simulation. The amount of each major element of typical concrete was cited from the reference. Specifically, the amount of each minor element was determined with an ICP-AES analysis.

Element	wt%	Element	wt%
H	0.45	Ca	7.8
Li*	3.8×10^{-4}	Ti	0.41
B*	4.4×10^{-4}	Mn*	0.28
O	48	Fe	2.5
Na	1.9	Co*	2.8×10^{-4}
Mg	0.86	Ni*	6.2×10^{-4}
Al	5.8	Cs*	6.8×10^{-5}
Si	29	Eu*	1.4×10^{-4}
S	0.091	Gd*	4.0×10^{-5}
K	2.6		

* very small amount but including for radioactivity analysis

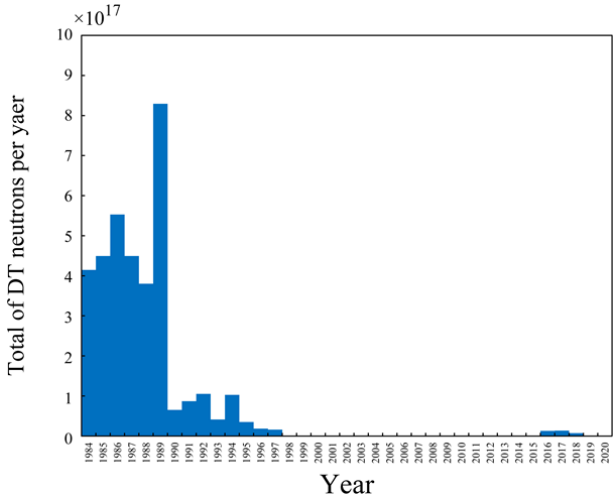

Fig. 2 Number of generated DT neutrons per year in the intense irradiation room. The number of generated neutrons is estimated from the operation records. The year of the maximum neutron generation was 1989. Since then, the use of the continuous neutron source had decreased significantly. From 1998 to 2015, the pulsed neutron source was primarily used to research double-differential cross-section measurements. The OKTAVIAN was not in operation from 2018 and 2020, owing to the malfunction caused by an earthquake of 6.1 Mj on June 18th, 2018.

Table 4 Elements in the accelerator components for the PHITS simulation.

Element	wt%
C	0.08
Si	1
Mn	2
P	0.045
S	0.03
Co	0.1
Ni	8
Cr	18
Fe	71

tively coupled plasma atomic emission spectroscopy (ICP-AES) analysis, which has been discussed in Sec. 4.2. To consider the neutron scattered by the accelerator, this simulation considered the accelerator body to be composed of stainless steel and copper. The productions of residual radionuclides with a half-life of longer than 100 days in concrete were investigated with the DCHAIN-SP. The major radionuclides are shown in Table 5. However, the two-dimensional (2D) distribution of radionuclides could not be directly obtained using the DCHAIN-SP; thus, the 2D distributions of the produced radionuclides were calculated with the tally of t-product in the PHITS. The radioactivities were evaluated based on the number of nu-

Table 5 Major radionuclides in the concrete wall.

Radionuclide	Half-life
^{3}H	12.32 years
^{14}C	5.7×10^{3} years
^{22}Na	2.6019 years
^{36}Cl	3.01×10^{5} years
^{39}Ar	269 years
^{41}Ca	1.03×10^{5} years
^{45}Ca	162.67 days
^{54}Mn	312.03 days
^{55}Fe	2.737 years
^{57}Co	271.74 days
^{60}Co	5.2713 years
^{59}Ni	1.01×10^{5} years
^{63}Ni	100.1 years
^{134}Cs	2.0648 years
^{152}Eu	13.537 years
^{154}Eu	8.593 years

clear interactions with decay constants and time differential equations with spatial resolution of 2D distributions being 1 cm. For example, the production of ^{152}Eu in concrete is based on ^{151}Eu(n,γ)^{152}Eu for thermal neutrons, and ^{153}Eu(n,2n)^{152}Eu for fast neutrons. This estimation is a simplified approach that does not consider daughter productions, although the daughter products of ^{152}Eu are ^{152}Gd (1.08×10^{4} y).

4. Experimental

4.1 Sample preparation

Core samples were cut with a diamond-core drill and from the concrete wall and floor of the intense irradiation room in December 2019, which was 17 months after the earthquake in 2018. The positions of obtained samples are shown in Fig. 1. Positions 1 and 2 were on the wall, while position 3 was on the floor below the Ti-T target, with distance between the Ti-T target and the floor being 180 cm. Core samples were 19 mm in diameter and 80 mm long. The average core sample density was approximately 2.3 g/cm^3. Each core sample was cut by 15 mm across and pulverized into 120 mesh ($\fallingdotseq$211 μm) particles with alumina mill.

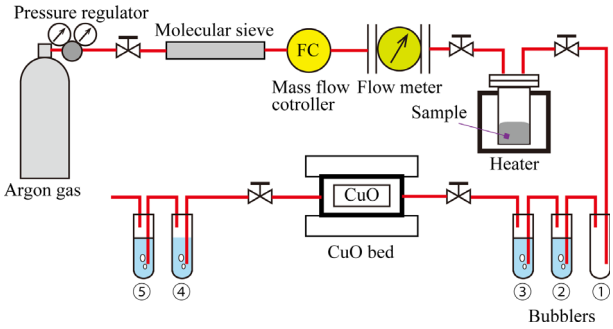

Fig. 3 Schematic of a tritium sampler system. The tritium sampler system is composed of an Ar gas flow system, a closed, stainless-steel container, an electric furnace, and water bubbling tubes. The core sample in the closed, stainless-steel container was heated by an electric furnace. The bubblers 1, 2, and 3 captured HTO, and 4 and 5 captured HT by oxidizing it to HTO in CuO oxidation beds. After mixing the trapped water with a liquid scintillator, the mixture was measured with a liquid scintillation counter.

4.2 ICP-AES analysis

Chemical composition of the concrete sample was analyzed employing ICP-AES. A core sample 1 g in weight was decomposed in 20 mℓ 6 N nitric acid within a high-pressure reactor at 190°C for 24 h. The sample was not completely dissolved, leaving a small amount of insoluble material. It was assumed that Li, B, K, Mn, Co, Ni, Gd, and Eu were completely soluble in the solution. The densities of the elements in the solution were analyzed using the ICP-AES system (ICPS-8000, Shimazu Corp., Japan).

4.3 Gamma-ray spectroscopy

In-situ gamma-ray in the irradiation room and gamma-ray emitted from core samples were measured using gamma-ray spectrometer. A handy high-purity Ge (HPGe) detector measuring 3 inches in diameter (1GC 40190, Princeton Gamma-Tech Instruments, Inc., USA) surrounded by lead shielding blocks was set in close contact with the wall at position 4 in Fig. 1, and consequently, the gamma-ray spectrum was acquired. The measurement time was approximately 2×10^{5} s.

Core samples were weighed and placed into a plastic container 54 and 64 mm in diameter and height, respectively. Subsequently, gamma-ray measurement was performed to determine the number of radionuclides using an HPGe detector (ORTEC, Inc., USA) with a measuring time of approximately 6×10^{5} s. Consequently, the radioactivities were determined from the gamma-ray spectra obtained using a library based on the table of radioactive isotopes. The detection efficiency of the HPGe detector was calibrated with standard radiation sources.

4.4 Tritium measurement

Figure 3 shows the schematic of a tritium sampler

system, which is composed of an Ar gas flow system, a closed stainless-steel container, an electric furnace, and water bubbling tubes [25–27]. The core sample weighing approximately 8 g in the closed, stainless-steel container was heated by an electric furnace at 400°C flowing Ar gas. Moisture in the Ar gas was removed via a 4A molecular sieve (GL Sciences Inc., Japan), which adsorbed molecules with effective diameter less than 0.4 nm (e.g., H_2O). The concentration of moisture and oxygen in the Ar gas was less than 1 ppm. Further, the Ar gas flow rates were fixed to be 25 sccm. Chemical forms of the released tritium were expected to be HTO (T_2O) and HT (T_2), which were captured separately using the two-stage water bubblers. The bubblers 1, 2, and 3 captured HTO, while 4 and 5 captured HT by oxidizing it to HTO in CuO oxidation beds. The calibration experiment was conducted by preparing concrete samples containing the known amounts of tritium. The detection efficiency for tritium in the concrete sample was determined to be 22% [28]. After mixing 1 mℓ of the trapped water with 10 mℓ of the liquid scintillator (EcoscintTM Ultra, National Diagnostics, UK), the mixture was measured with a liquid scintillation counter (LSC-5100, Hitachi Ltd., Japan). The detection limit of tritium in the core samples was approximately 1.8 Bq/g.

Furthermore, the smear measurement for surface contamination with tritium on the wall was performed. A part of the wall in the intense irradiation room was wiped off with a smear filter paper (ADVANTEC, Japan). Thereafter, the liquid scintillator, including the smear filter paper, was analyzed via the liquid scintillation counter. The wiping

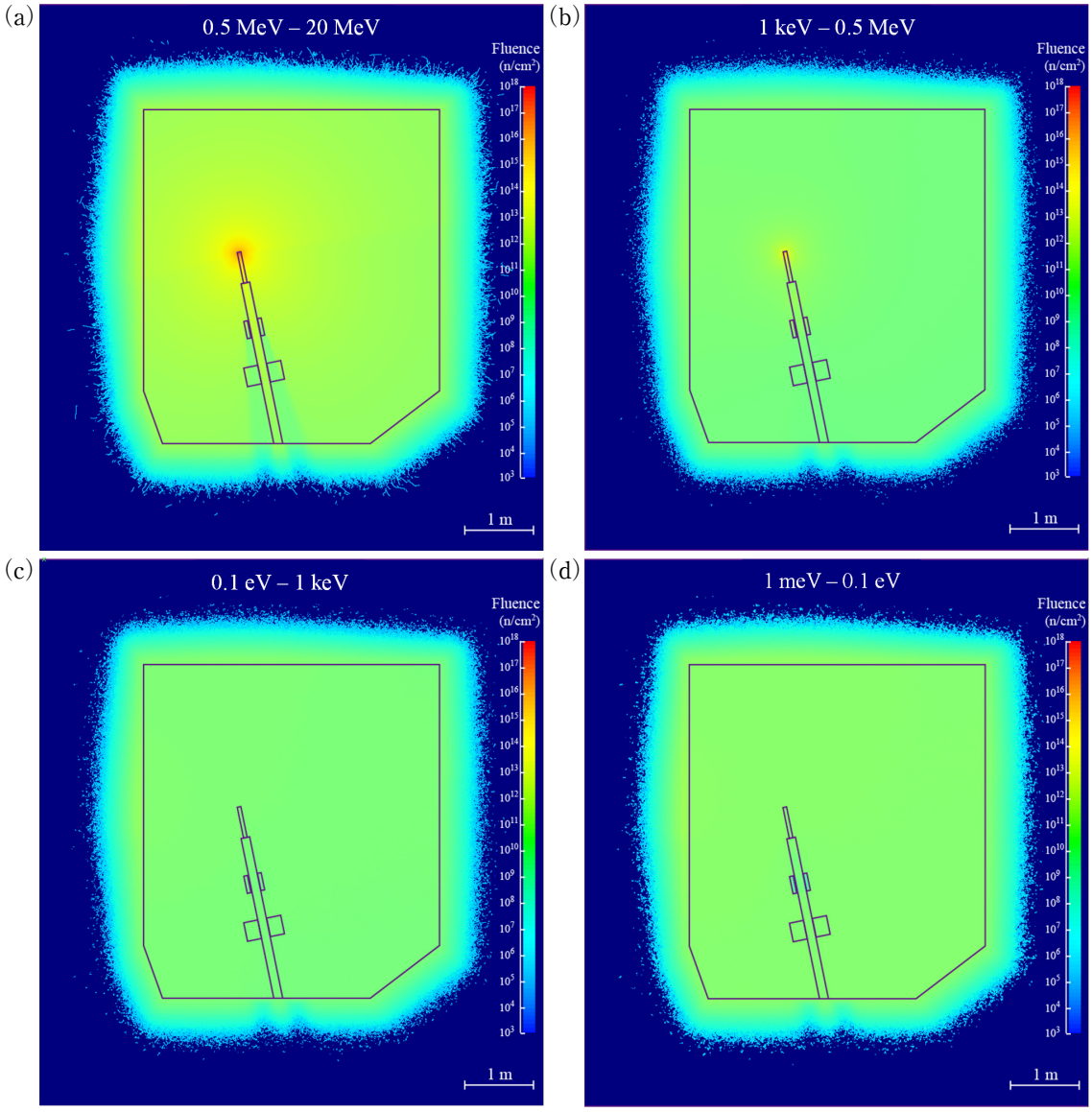

Fig. 4 2D maps of neutron fluences were calculated by the PHITS. The neutron energy ranges are (a) DT (0.5 - 20 MeV), (b) fast (1 keV - 0.5 MeV), (c) epithermal (0.1 eV - 1 keV), and (d) thermal (1 meV - 0.1 eV). DT and fast neutrons spread radially at the center of the Ti-T target. The fluence distributions of epithermal and thermal neutrons were almost uniform due to neutron moderations.

efficiency was assumed as 10% to evaluate the tritium radioactivity conservatively.

5. Results and Discussion

5.1 Simulation

Figure 4 shows the 2D maps of neutron fluences in different energy ranges. DT neutrons (0.5 MeV - 20 MeV) spread radially at the center of the Ti-T target, and the fast neutrons (1 keV - 0.5 MeV) spread as well as the DT neutrons. Further, the fluence distributions of epithermal (0.1 eV - 1 keV) and thermal neutrons (1 meV - 0.1 eV) were almost uniform due to neutron moderations in the concrete wall and accelerator body. Figure 5 shows the energy spectrum of the neutron at position 1, showing an intense peak at 14 MeV and a broad peak between 1 meV and 0.1 eV. The production of radionuclides for fast neutron interactions were primarily (n,2n), (n,p), (n,α), (n,d), and (n,t); while that for the epithermal and thermal neutron interactions was based on neutron captures (n,γ).

Figure 6 shows the time histories of each radioactivity at position 1. The radioactivity was estimated by the DCHAIN-SP. The fluctuations of radioactivities were related to the total of generated neutrons per year and its decay constants. The radionuclides of ^{41}Ca, ^{45}Ca, ^{60}Co, and ^{152}Eu were produced by thermal neutron capture reactions, such as ^{40}Ca(n,γ)^{41}Ca, ^{44}Ca(n,γ)^{45}Ca, ^{59}Co(n,γ)^{60}Co, and ^{151}Eu(n,γ)^{152}Eu, respectively. In contrast, those of ^{22}Na, ^{54}Mn, ^{55}Fe, and ^{152}Eu and were produced by fast neutron reactions, such as ^{23}Na(n,2n)^{22}Na, ^{55}Mn(n,2n)^{54}Mn, ^{56}Fe(n,2n)^{55}Fe, and ^{153}Eu(n,2n)^{152}Eu, respectively. The maximum radioactivity observed was in 1989 at the maximum number of generated DT neutrons. Thereafter, radioactivities decreased between 1989 and 2014 according to decay constants. The radioactivities of ^{45}Ca and ^{54}Mn, which have short half-lives, were high in the early stage and then drastically decreased. Moreover, the radioactivities with half-lives on the order of 10 years, such as ^{3}H, ^{60}Co, and ^{152}Eu, were gradually decreased.

Figure 7 shows the 2D distributions of the radioactivities of ^{3}H, ^{22}Na, ^{26}Al, ^{36}Cl, ^{41}Ca, ^{45}Ca, ^{54}Mn, ^{55}Fe, ^{57}Co, ^{60}Co, ^{59}Ni, ^{63}Ni, ^{152}Eu, and ^{154}Eu for the concrete at the floor surface. The 2D distributions of the radioactivities based on the neutron capture reactions, such as ^{3}H and ^{60}Co, were approximately uniform. Figure 8 shows the depth profile of ^{152}Eu radioactivity density at position 1. The maximum radioactivity density of ^{152}Eu was approximately 9 cm. Figure 9 shows the depth profile of tritium radioactivity density at position 1 and the depth profile is similar to that of ^{152}Eu radioactivity.

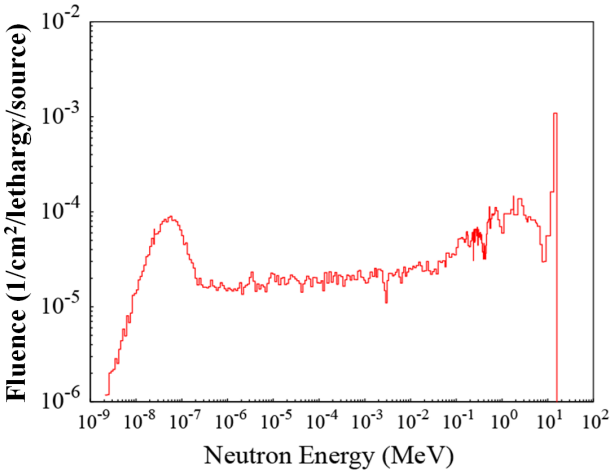

Fig. 5 Energy spectrum of the neutron at position 1 calculated by the PHITS. The energy spectrum has an intense peak at 14 MeV and a broad peak between 1 meV and 0.1 eV.

5.2 Gamma-ray spectroscopy

Figure 10 shows the gamma-ray spectrum measured by the HPGe detector set on the wall in the intense irradiation room. Major radionuclides produced by neutrons were ^{22}Na, ^{54}Mn, ^{60}Co, and ^{152}Eu (except for natural radionuclides such as ^{40}K, ^{208}Tl, ^{214}Pb, ^{214}Bi, ^{226}Ra, ^{228}Ac, and ^{235}U). ^{55}Fe could not be confirmed as the emitted X-ray energy of ^{55}Fe is 0.06 MeV and the clearance level of ^{55}Fe is 1000 Bq/g [29]. As this energy spectrum clearly included ^{60}Co gamma-rays, it appeared that gamma-rays from the accelerator body were also detected.

The radioactivity of ^{152}Eu was suitable for comparing

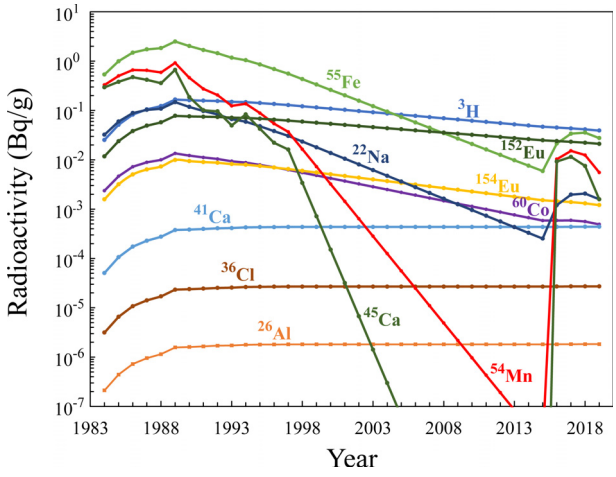

Fig. 6 Changes in the radioactivity over time at position 1. The radioactivity was estimated by the DCHAIN-SP. The fluctuations of radioactivity were dependent on the total number of neutrons per year and its decay constant. The radioactivity was at its maximum in 1989 and at the maximum amount of DT neutrons. The radioactivity decreased between 1989 and 2014, according to the decay constant. The radioactivities of ^{45}Ca and ^{54}Mn, which have short half-lives, were high in the early stage and subsequently decreased drastically. The radioactivities with half-lives on the order of 10 years, such as ^{3}H, ^{60}Co, and ^{152}Eu, were gradually decreased.

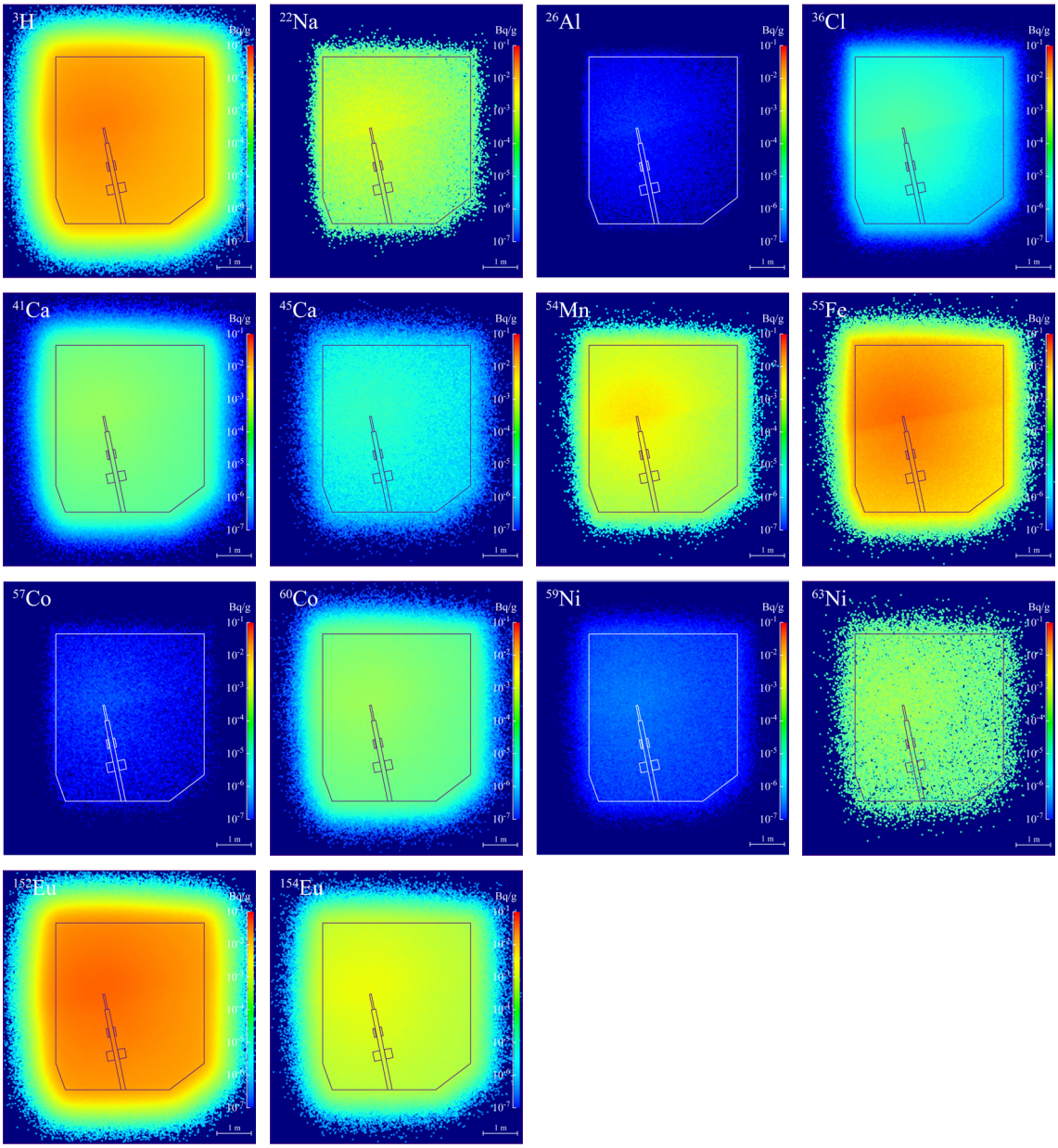

Fig. 7 2D distributions of radioactivities of ^{3}H, ^{22}Na, ^{26}Al, ^{36}Cl, ^{41}Ca, ^{45}Ca, ^{54}Mn, ^{55}Fe, ^{57}Co, ^{60}Co, ^{59}Ni, ^{63}Ni, ^{152}Eu, and ^{154}Eu for the concrete at the floor surface.

experimental and calculated results. Table 6 summarizes the radioactivities of core samples for ^{152}Eu at three positions. The experimental and simulation results were somewhat consistent with no large differences being observed. The radioactivity was approximately one-fifth of the clearance level of ^{152}Eu, that is, 0.1 Bq/g.

5.3 Tritium measurement

Table 7 shows the radioactivities of tritium at three positions. All the radioactivities were much smaller than the clearance level of tritium (i.e., 100 Bq/g). However, the experimental results values near the surface of the concrete wall are larger than those of the simulation results. Further, all radioactivities over 1.5 cm in depth were under the lower detection limit - 1.8 Bq/g. This discrepancy indicated that the tritium contamination on the wall was caused by tritium leaked from the Ti-T target. Therefore, the smear measurement investigated the tritium contamination on the wall in the intense irradiation room. Figure 11 shows the results of the smear measurement. There were a few highly contaminated regions observed. The maximum tritium density was 30 Bq/cm^2 at position 5. A core sample at position 5 was obtained after the surface was completely wiped off with wet Kimwipes (Nippon Paper Crecia Corp., Japan) and analyzed using the tritium sampler system. The tritium density of the core sample was under the lower detection limit, as shown in Table 8. Thus, this result indicated that the tritium diffused from the Ti-T

target was only attached to the surface of the concrete wall and most of the tritium did not penetrate the concrete wall.

6. Conclusions

We investigated the radioactivation of the concrete wall of an intense DT neutron irradiation room in a fast neutron generator facility. The radioactivation and tri-

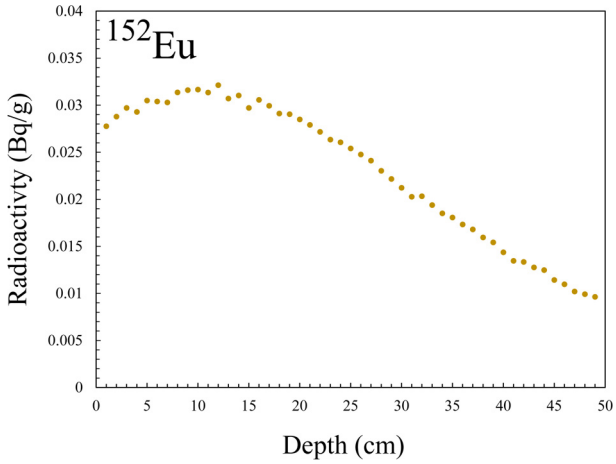

Fig. 8 Depth profile of ^{152}Eu radioactivity at position 1 calculated by PHITS. Radioactivity of ^{152}Eu increases with depth from the surface, maximizing at approximately 9 cm and then decreasing.

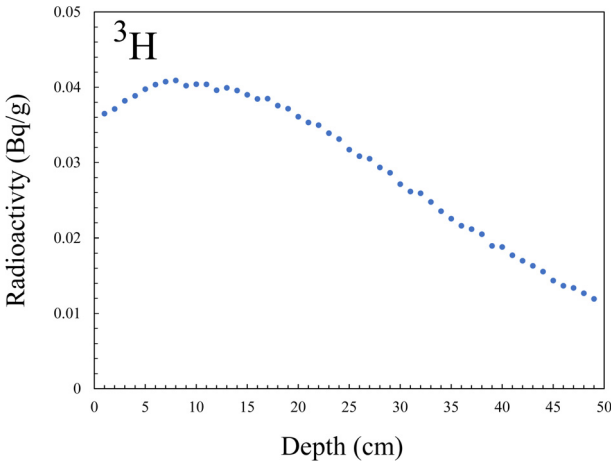

Fig. 9 Depth profile of tritium radioactivity at position 1 calculated by PHITS. Radioactivity of tritium increases with depth from the surface, maximizing at approximately 8 cm and then decreasing.

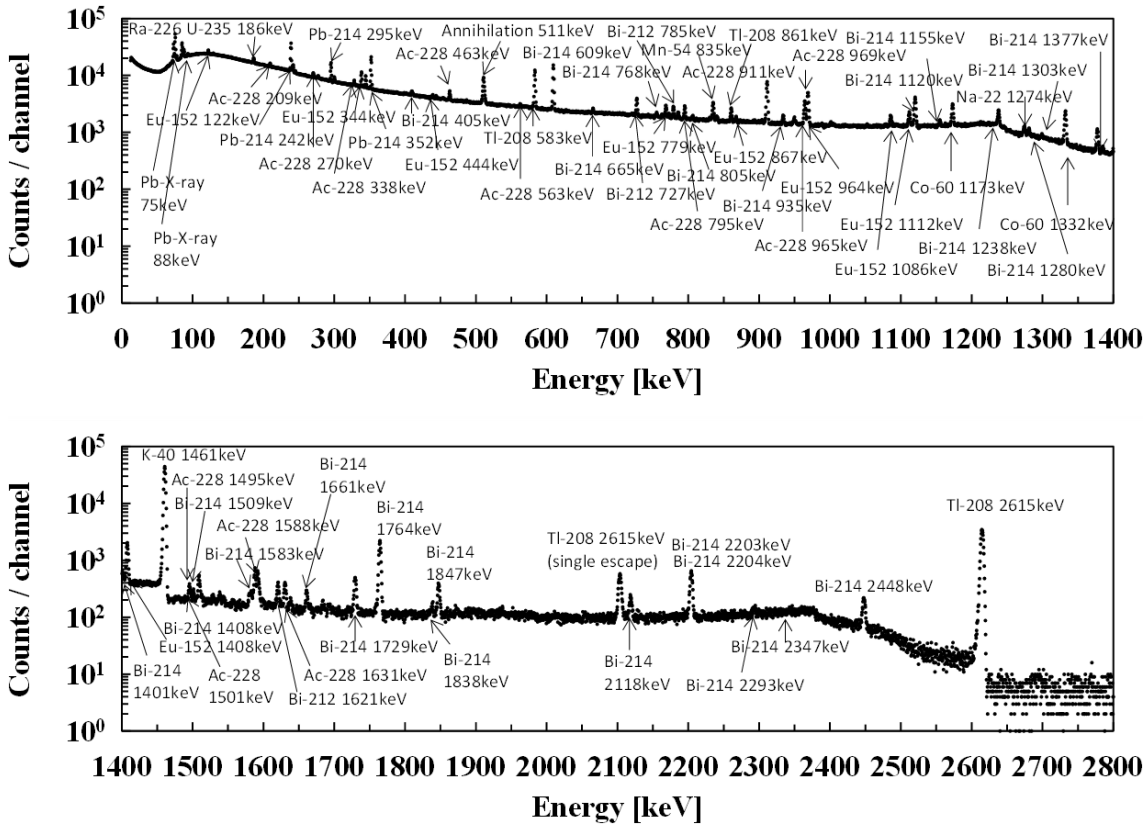

Fig. 10 Gamma-ray spectroscopy on the wall in the intense irradiation room at position 4. Major radionuclides generated by neutrons are ^{22}Na, ^{54}Mn, ^{60}Co, and ^{152}Eu.

Table 6 Radioactivity of core samples for ^{152}Eu. The experimental and simulation results do not show a significant difference.

Depth (cm)	Position 1		Position 2		Position 3	
	Exp.	Sim.	Exp.	Sim.	Exp.	Sim.
0.0–1.5	2.8	2.7	1.4	1.6	2.8	2.2

Table 7 Radioactivities of core samples for tritium. The experimental results at the surface of the concrete wall are larger than the simulation results. All radioactivities over 1.5 cm depth were under the lower detection limit −1.8 Bq/g.

Depth (cm)	Position 1		Position 2		Position 3	
	Exp.	Sim.	Exp.	Sim.	Exp.	Sim.
0.0–1.5	3.3	0.037	2.1	0.030	N.D.	0.032
1.5–3.0	N.D.	0.038	N.D.	0.029	N.D.	0.033
3.0–4.5	N.D.	0.039	N.D.	0.027	N.D.	0.034
4.5–6.0	N.D.	0.040	N.D.	0.026	N.D.	0.035
6.0–7.5	N.D.	0.040	N.D.	0.025	N.D.	0.035

Detection limit is 1.8 Bq/g.

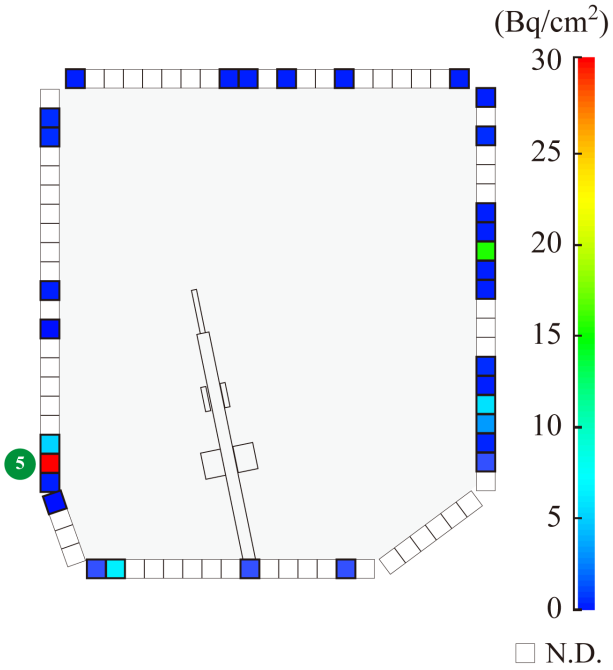

Fig. 11 Results of the smear measurement. There were a few highly contaminated regions. The maximum tritium density is 30 Bq/cm^2.

Table 8 Radioactivity of the core sample at the maximum position for smear measurement after the tritium on the wall was completely wiped off. The tritium density of the core sample was below the lower detection limit.

Depth (cm)	Position 5	
	Exp.	Sim.
0.0–1.5	N.D.	0.034

tium contamination for the parts of the accelerator body are serious problems of radioactive waste. Core samples of the concrete wall were collected at various positions and the residual radionuclides in them were determined via gamma-ray spectrometry. Major long-lived radionuclides determined were T, ^{55}Fe, ^{54}Mn, ^{60}Co, and ^{152}Eu. The radioactivity of ^{152}Eu is possibly consistent with the result obtained with the neutron transport simulation code. Further, the radioactivities of ^{54}Mn and ^{60}Co were smaller, compared to that of ^{152}Eu.

The amount of tritium in the core sample was measured using a tritium sampler system, which was composed of an Ar gas flow system, a closed, stainless-steel container, an electric furnace, and water bubbling tubes. The amount of tritium determined in all core samples near

the wall's surface was two orders of magnitude higher than the simulation results. However, the tritium diffused from the Ti-T target was only attached to the surface of the concrete wall and most of the tritium did not penetrate the wall. Moreover, the contamination of tritium inside the concrete wall of the intense irradiation room was sufficiently small.

The results of the radioactivation of the fast neutron generator facility are expected to aid in maintaining the operation of the facility and its eventual decommission.

Acknowledgments

The authors are extremely grateful to Hisashi Sugimoto and Jun Datemichi of the OKTAVIAN staff for the careful operation and maintenance of OKTAVIAN for many years. Valuable suggestions regarding the sample preparation were provided by Masaki Tokai of Osaka University.

[1] M.Z. Youssef and R.W. Conn, Nuclear technology/fusion **3** (3), 361 (1983).
[2] S. Fetter *et al.*, Fusion Eng. Des. **6**, 123 (1988).
[3] E.T. Cheng, Fusion Eng. Des. **10**, 231 (1989).
[4] Y. Ikeda *et al.*, Fusion Eng. Des. **18**, 387 (1991).
[5] H. Freiesleben *et al.*, Fusion Eng. Des. **42** (1-4), 337 (1998).
[6] M. Ohta *et al*., Final results of IRDFF benchmark test at JAEA/FNS. No. INDC (NDS)–0731. 2017.
[7] M. Martone *et al*., J. Nucl. Mater. **212,** 1661 (1994).
[8] S. Fiore *et al*., 2016 IEEE Nuclear Science Symposium, Medical Imaging Conference and Room-Temperature Semiconductor Detector Workshop (NSS/MIC/RTSD), 2016, pp. 1-3.
[9] K. Sumita *et al.*, Nucl. Sci. Eng. **106** (3), 249 (1990).
[10] K. Masumoto *et al.*, Radiation Safety Management **20**, 1 (2021).
[11] K. Masumoto *et al.*, J. Radioanal. Nucl. Chem. **255** (3), 465 (2003).
[12] K. Bessho *et al.*, Nucl. Instrum. Methods Phys. Res. B **259**, 702 (2007).
[13] Q.B. Wang *et al.*, J. Radioanal. Nucl. Chem. **273** (1), 55 (2007).
[14] A. Brusa *et al.*, Med. Phys. **35** (7), 3049 (2008).
[15] K. Masumoto *et al.*, J. Radioanal. Nucl. Chem. **278**, 449 (2008).
[16] L. Ulrici and M. Magistris, Radiat. Prot. Dosim. **137** (1-2), 138 (2009).
[17] C. Bungau *et al.*, Phys. Rev. Special Topics - Accelerators and Beams **17**, 084701 (2014).
[18] E. Waller *et al.*, Health Phys. **113**(3), 227 (2017).
[19] S. Vichi *et al.*, Radiat. Phys. Chem. **161**, 48 (2019).
[20] C. Duchemin *et al.*, Nucl. Instrum. Methods Phys. Res. A **919**, 42 (2019).
[21] G. Yoshida *et al.*, Radiation Safety Management **20**, 1 (2021).
[22] H.L. Swami *et al.*, Fusion Eng. Des. **165**, 112229 (2021).
[23] T. Sato *et al.*, J. Nucl. Sci. Technol. **11** (1), 86 (2012).
[24] H. Miyano *et al*., *Monitoring for Compliance with Clearance Level*: 2005, (Atomic Energy Society of Japan, Japan) p. 172. (in Japanese).
[25] K. Kumagai *et al.*, Fusion Eng. Des. **136**, 1269 (2018).
[26] K. Kumagai *et al.*, Plasma Fusion Res. **13**, 3404071 (2018).
[27] K. Kumagai *et al.*, Plasma Fusion Res. **14**, 1405044 (2019).
[28] J. Duda *et al*., J. Environ. Radioact. **189**, 236 (2018).
[29] H. Miyano *et al*., *Monitoring for Compliance with Clearance Level*: 2005, (Atomic Energy Society of Japan, Japan) p. 16. (in Japanese).